

**AD-A267 027**



②

**NASA Contractor Report 191458**

**ICASE Report No. 93-20**

# ICASE



## **SOME ASPECTS OF THE AEROACOUSTICS OF HIGH-SPEED JETS**

**Sir James Lighthill**

DTIC  
ELECTE  
JUL 23 1993  
S B D

NASA Contract No. NAS1-19480  
May 1993

Institute for Computer Applications in Science and Engineering  
NASA Langley Research Center  
Hampton, Virginia 23681-0001

Operated by the Universities Space Research Association



DISTRIBUTION STATEMENT A  
Approved for public release;  
Distribution Unlimited

National Aeronautics and  
Space Administration

Langley Research Center  
Hampton, Virginia 23681-0001

**93-16584**



47px

93 7 22 000

## ICASE Fluid Mechanics

Due to increasing research being conducted at ICASE in the field of fluid mechanics, future ICASE reports in this area of research will be printed with a green cover. Applied and numerical mathematics reports will have the familiar blue cover, while computer science reports will have yellow covers. In all other aspects the reports will remain the same; in particular, they will continue to be submitted to the appropriate journals or conferences for formal publication.

DTIC QUALITY INSPECTED 1

<b>Accession For</b>	
NTIS GRA&I	<input checked="checked" type="checkbox"/>
DTIC TAB	<input type="checkbox"/>
Unannounced	<input type="checkbox"/>
Justification	
By	
Distribution/	
Availability Codes	
Dist	Avail and/or Special
A-1	

# SOME ASPECTS OF THE AEROACOUSTICS OF HIGH-SPEED JETS<sup>1</sup>

*Sir James Lighthill*  
Mathematics Department  
University College London  
Gower Street  
London WC1E 6BT  
ENGLAND

## ABSTRACT

The Lecture begins by sketching some of the background to contemporary jet aeroacoustics. Then it reviews scaling laws for noise generation by low-Mach-number airflows and by turbulence convected at "not so low" Mach number. These laws take into account the influence of Doppler effects associated with the convection of aeroacoustic sources.

Next, a uniformly valid Doppler-effect approximation exhibits the transition, with increasing Mach number of convection, from compact-source radiation at low Mach numbers to a statistical assemblage of conical shock waves radiated by eddies convected at supersonic speed. In jets, for example, supersonic eddy convection is typically found for jet exit speeds exceeding twice the atmospheric speed of sound.

The Lecture continues by describing a new dynamical theory of the nonlinear propagation of such statistically random assemblages of conical shock waves. It is shown, both by a general theoretical analysis and by an illustrative computational study, how their propagation is dominated by a characteristic "bunching" process. That process – associated with a tendency for shock waves that have already formed unions with other shock waves to acquire an increased proneness to form further unions – acts so as to enhance the high-frequency part of the spectrum of noise emission from jets at these high exit speeds.

---

<sup>1</sup>This is the original version of the Theodorsen Lecture which was supported by the Institute for Computer Applications in Science and Engineering (ICASE) and the National Aeronautics and Space Administration (NASA), Langley Research Center, Hampton, VA 23681-0001 under NASA Contract No. NAS1-19480.

## 1. Introduction

I warmly appreciate the invitation to give the inaugural Theodorsen Lecture in honor of a renowned Langley scientist, Theodore Theodorsen. It is moreover a very special pleasure for me to pay tribute here to the deep and intricate aerodynamic researches of Dr Theodorsen because they powerfully influenced all work on airfoil design during the early 1940s and, in particular, some extensive activities in this field pursued by the team in the NPL Aerodynamics Division, under Sydney Goldstein's leadership, of which I then formed part. This team's achievements were later to be comprehensively expounded by Dr Goldstein in his Wright Brothers Lecture (Goldstein 1948), where he went out of his way to stress the fundamental importance of Theodore Theodorsen's key contributions to airfoil theory and to airfoil design.

By that time, in the late 1940s, I myself was starting work on a rather new branch of aerodynamics, which I then called the study of sound generated aerodynamically (Lighthill 1952) and which came later to be known as aeroacoustics. From the outset a vitally important branch of aeroacoustics was concerned with the noise of turbulent jets, a subject to which I was to devote my own Wright Brothers Lecture (Lighthill 1963).

Fundamental investigations of turbulent flows had, of course, been yet another of the major interests pursued by Theodore Theodorsen. I have accordingly felt that a lecture concerned with turbulent jets and with one of the gravest environmental problems posed by their use for aircraft propulsion purposes — namely, the noise they generate — would form a fitting memorial tribute to that great aerodynamicist.

Furthermore, a lecture on this theme is particularly appropriate to an important occasion here at Langley; where early pioneering researches on aeroacoustics, including some crucial experiments on jet noise, were carried out

by Harvey Hubbard and others (Lassiter & Hubbard 1952). Last year, moreover, ICASE and NASA Langley Research Center joined forces to host an exceptionally fine Workshop, which gave an authoritative view of the past, present and future of aeroacoustics, with special emphasis on Computational Aeroacoustics. This Workshop looked forward towards "a second golden age of aeroacoustics", in which both new theoretical and new computational approaches, closely linked to new experimental techniques, would be employed in response to the challenge of those toughened environmental requirements that are now to be imposed on all new aircraft designs (Hussaini & Hardin 1993).

I personally was delighted to participate in this workshop by giving an introductory lecture looking back to some of the earlier fundamental discoveries in aeroacoustics, as well as by chairing the Final Panel Discussion which looked forward to likely future developments as aeroacoustics enters its second golden age. In between, I was stimulated by hearing many brilliant contributions concerned with meeting some of those new challenges to which I just referred.

One of the most exciting of these is posed by the US High Speed Civil Transport project (HSCT), an extremely promising plan for a supersonic transport aircraft ingeniously designed to minimise the level of supersonic-boom annoyance. However the corresponding problems of reducing engine noise for such an aircraft to within acceptable limits raise some thorny questions and may, in particular, demand that a fundamental aeroacoustic analysis of jets at relatively high speed be undertaken.

In a purely aeroacoustical context the appropriate definition of the Mach number  $M$  of a jet is the ratio of its exit speed  $U$  to the speed of sound  $c_0$  in the atmosphere into which it is radiating. Now, the general trend of aeroacoustic Mach numbers for civil aero-engines (in other words, for the engines of those aircraft which face the greatest aeroacoustic challenges) has been a downward trend for very many years, and this has allowed engines to become simultaneously quieter

and more powerful because in a wide range of Mach numbers (see figure 1 below) the ratio  $\eta$  of acoustic power radiated to jet power delivered varies as  $M^2$ . At lower jet Mach numbers, then, noise radiated can be less even though jet power is greater.

Evidently, it has only been the introduction of aeroengines of ever larger and larger diameter that has permitted such increased engine powers to be delivered at the necessary low noise levels by means of this downward trend in jet Mach number. For a supersonic aircraft, on the other hand, the use of extra-wide engines is out of the question because their supersonic-boom emissions, and also the associated shock-wave drag, would be unacceptably great. Such considerations rule out any similar reduction in jet Mach number in this case.

It follows that work on engine-noise reduction for the HSCT project has been calling for many new fundamental studies of the generation of noise by jets at relatively high Mach numbers. This is the range of values of  $M$  in excess of 2 for which (see figure 1 below) the proportion  $\eta$  of jet power that is converted into noise approaches an asymptotic value of 0.01 or a little less. Moreover the noise field has become highly directional, because the turbulent eddies that generate sound are themselves being convected at supersonic speeds so that they emit their own supersonic booms in the Mach direction defined by an eddy convection velocity and the atmospheric speed of sound (Ffowcs Williams & Maidanik 1965).

In an actual aero-engine installation, of course, there may be a great difference between the pure noise field of the high-speed jet itself and the overall noise radiated from the installation taken as a whole. However, an essential prerequisite for designing that installation so as to bring down ground noise levels is to understand as well as possible the primary noise field generated by the high-speed jet. This is why so many stimulating lectures contributed to last year's Workshop at Langley (Hussaini & Hardin 1993) were devoted to different aspects of that primary noise generation.

In this Theodorsen Lecture, the main material which I shall present describes certain new researches into which I was drawn as a direct result of listening to all those stimulating contributions which, as I have indicated, were concerned with how the high-speed jet generates a noise field emitted largely in the Mach direction. In fact the qualifying phrase which appears in my title "Some aspects of the aeroacoustics of high-speed jets" is mainly intended to recognize that noise-generation mechanisms in such jets have long been studied and, above all, are being investigated actively today. Accordingly I shall refer only briefly to those generation aspects of the problem and concentrate rather on some other aspects which appear, relatively speaking, to have been neglected.

These aspects of the aeroacoustics of high-speed jets on which I shall concentrate are related to those effects of nonlinear sound propagation which immediately start to modify the noise field once it has been generated. Such nonlinear propagation effects may readily be expected to be important from that analogy with supersonic-boom generation which I already mentioned; and which tends to suggest that each supersonically convected eddy will emit in the Mach direction a boom-like signal that should include one or more conical shock waves. Accordingly a random sequence of eddies should generate a random, thickly packed assemblage of conical shock waves, and this idea is supported by various experimental, theoretical and computational studies.

My lecture, then, is primarily concerned with the nonlinear acoustic propagation of such random assemblages of conical shock waves once they have been formed. Thus it includes a study of the inherent tendency of the shock strengths to decay (through conical spreading and internal dissipation), as opposed by increases in strength that occur whenever adjacent shock waves unite. A certain "bunching" tends to arise, because a union of two adjacent shocks is found to increase the likelihood of further union with other neighbouring shocks. The high-frequency part of the noise spectrum is made more intense than would otherwise be the case by these bunching tendencies.

A completely general theoretical analysis is used to demonstrate the universal tendency towards bunching. Then a computational study is carried out in order to exemplify details of the process, which is expected to be important for the appreciation of how Mach wave fields are modified in the region of conical propagation that surrounds a high-speed jet.

All of this new material concerned with nonlinear propagation is preceded, however, by a simplified summary account of how jet noise is generated. This account — broadly along the lines of my Wright Brothers Lecture — shows how some sort of continuous transition can be discerned between more familiar processes of jet-noise generation at relatively low Mach number and that generation of a random assemblage of conical shock waves which sets in at the higher jet Mach numbers.

Next, a well known transformation of coordinates (Whitham 1956, Lighthill 1978) is used to reduce the problem of conical propagation, concerned with how a *temporal* waveform varies with distance  $r$  along the Mach direction, into a plane-wave problem. In this latter problem the time  $t$  replaces  $r^{1/2}$ , and attention is focussed on how a given spatial waveform varies with time.

The spatial waveform that needs to be studied in this latter context turns out to be a spatially unlimited assemblage of random "sawtooth" waves, of the type (see figure 2 below) into which a general plane sound wave of large amplitude would evolve during a certain time  $t$ . It consists of randomly located shocks (with random strengths) separated by expansion waves in which the slope of excess signal velocity as a function of position takes the value  $1/t$ .

I shall present a new and quite general theory of the nonlinear dynamics of random sawtooth waves. It shows how the inherent tendency of the shock strengths themselves is to decay like  $1/t$  but that this tendency is opposed whenever shocks unite with adjacent shocks. Moreover those "bunchings" of unions to which



I already referred combine in a sort of "snowball" effect to make major modifications in the waveform.

After a transformation back into the original variables describing conical propagation,  $t$  is replaced by  $r^{3/4}$  but predicted shock strengths have to be divided by a further  $r^{3/4}$  factor. Thus the inherent tendency of the shock strengths is now to decay like  $1/r$  but we shall yet again find that this tendency is powerfully opposed by those "bunching" effects whose special relevance, in a noise context, is to intensify the high-frequency part of the jet noise spectrum.

## 2. Scaling of aerodynamic noise at low Mach number

An airflow of characteristic velocity  $U$  and length-scale  $L$ , with high enough Reynolds number  $\rho UL/\mu$  (where  $\rho$  and  $\mu$  are the air's density and viscosity), is a turbulent airflow. The chaotic sound field which it radiates through the surrounding atmosphere (with undisturbed sound speed  $c_0$ ) is known as aerodynamic noise.

This sound radiation — apart from any effects of solid boundaries (see below) — is precisely that which would be generated by quadrupole sources of strength  $T_{ij}$  per unit volume (Lighthill 1952, 1978), where  $T_{ij}$  stands for the difference between the momentum flux in the real airflow and that in a simple acoustic medium with sound speed  $c_0$ . The most important term in  $T_{ij}$  is the convective flux  $\rho u_i u_j$  of a momentum component  $\rho u_i$  carried by a velocity component  $u_j$ .

Turbulent airflows at low Mach number  $U/c_0$  are compact sources of aerodynamic noise because typical frequencies  $\omega$  in the turbulence scale as  $U/L$  (Strouhal scaling) and therefore the compactness ratio  $\omega L/c_0$  is small (Lighthill 1962). It means that differences in phases of emission for sounds reaching a

distant observer are small enough for the whole flow field to radiate effectively as a single source.

This source may be of dipole type, with dipole strength  $F_i$ , in cases when the vector  $F_i$  represents a force acting between the turbulent airflow and a solid body immersed in it (Curle 1955, Ffowcs Williams & Hawkings 1969). Typically,  $F_i$  scales as  $\rho U^2 L^2$ , so that its rate of change scales as  $\rho U^3 L$ ; and then the radiated power

$$\langle \dot{F}_i^2 \rangle / 12\pi \rho c_o^3 \quad (1)$$

scales as  $\rho U^6 L^2 / c_o^3$ : a sixth-power dependence on flow speed. Also, the acoustic efficiency  $\eta$ , defined as the ratio of radiated power to a rate of delivery (proportional to  $\rho U^3 L^2$ ) of energy to the flow, scales as  $(U/c_o)^3 = M^3$ .

On the other hand turbulent airflows at low Mach number in the absence of any such solid body radiate effectively as a single quadrupole source, with total strength  $Q_{ij}$  scaling as  $\rho U^2 L^3$  (because the strength  $T_{ij}$  per unit volume scales as  $\rho U^2$ ). The acoustic intensity at a distant point, whose vector separation and scalar distance from the source are  $x_i$  and  $r$  respectively, is then

$$\langle (\ddot{Q}_{ij} x_i x_j / r^2)^2 \rangle / 16\pi^2 r^2 \rho c_o^5, \quad (2)$$

where the second time-derivative  $\ddot{Q}_{ij}$  scales as  $\rho U^4 L$ . Accordingly, the radiated power scales as  $\rho U^8 L^2 / c_o^5$  (an eighth-power dependence on flow speed; see Lighthill 1952, 1962) and the acoustic efficiency  $\eta$  scales as  $(U/c_o)^5 = M^5$ .

At low Mach numbers, therefore, such aerodynamic noise radiation of quadrupole type is unimportant whenever dipole radiation due to fluctuating body force (with efficiency proportional to  $M^3$ ) is also present (Crighton 1975). In other problems, however, such as the noise of a jet (with practically no fluctuating body force), the quadrupole source becomes dominant. For example, a turbulent jet of exit speed  $U$  radiates with an acoustic efficiency of order  $10^{-4}(U/c_o)^5$ .

### 3. Aerodynamic noise at not so low Mach number

The chaotic nature of turbulent flow implies that velocity fluctuations at points  $P$  and  $Q$ , although they are well correlated when  $P$  and  $Q$  are very close, become almost uncorrelated when  $P$  and  $Q$  are not close to one another. Here we recall that the correlation coefficient  $C$  between velocities  $u_P$  and  $u_Q$  is defined as

$$C = \langle v_P \cdot v_Q \rangle / \langle v_P^2 \rangle^{1/2} \langle v_Q^2 \rangle^{1/2} \quad (3)$$

in terms of the deviations  $v_P = u_P - \langle u_P \rangle$  and  $v_Q = u_Q - \langle u_Q \rangle$  from their means. When two uncorrelated quantities are combined, their mean square deviations are added up:

$$\langle v_P + v_Q \rangle^2 = \langle v_P^2 \rangle + \langle v_Q^2 \rangle \text{ if } C = 0 \quad (4)$$

(because the term  $2\langle v_P \cdot v_Q \rangle$  vanishes).

Theories of turbulence define a correlation length  $\ell$ , with  $C$  not far from 1 ( $u_P$  and  $u_Q$  well correlated) when  $PQ$  is substantially less than  $\ell$ , and  $C$  not far from zero ( $u_P$  and  $u_Q$  almost uncorrelated) when  $PQ$  substantially exceeds  $\ell$ . Roughly speaking, different regions of size  $\ell$  ("eddies") generate uncorrelated sound fields, and the mean square radiated noise is the sum of the mean square outputs from all of the regions (Lighthill 1954, 1962).

Typical frequencies  $\omega$  in the turbulence are of order  $\omega = v/\ell$ , where  $v$  is a typical root mean square velocity deviation  $\langle v^2 \rangle^{1/2}$ . For each region of size  $\ell$ , therefore, the compactness condition that  $\omega\ell/c_o$  be small is satisfied when  $v/c_o$  is small.

Compactness, then, requires only that a root mean square velocity deviation  $v$ , rather than a characteristic mean velocity  $U$ , be small compared with  $c_o$ . The associated restriction on  $U/c_o$  is less and can be satisfied at "not so low" Mach number.

On the other hand the sound radiated is no longer that of a single quadrupole source. Rather it is a combination of uncorrelated radiation patterns from different regions of size  $\ell$ , each with an intensity field (2) where  $Q_y = \ell^3 T_y$ ; while by equation (4) the intensity fields of different regions may simply be added. Therefore, on division by the volume  $\ell^3$  of a region, we obtain the intensity pattern radiated per unit volume of turbulence as

$$\ell^3 \langle (\ddot{T}_y x_i x_j r^{-2})^2 \rangle / 16\pi^2 r^2 \rho c_o^5. \quad (5)$$

#### 4. Doppler effects on frequency, volume and compactness

Moreover the radiation from any single eddy is subject to a modification — the Doppler effect — as a result of the eddy being convected at "not so low" Mach number. A rather familiar element of Doppler effect on the radiation pattern of a moving source of sound is its shift in frequency, but there are changes also in its effective volume, and in its compactness.

All of these Doppler effects on the sound received by an observer at a far-field location depend not on the speed  $V$  with which the source moves but on its velocity component  $w$  in the direction of the observer. In the case of an observer located on a line making an angle  $\Theta$  with a source's direction of motion at speed  $V$ , this velocity component  $w$  has the form

$$w = V \cos \theta. \quad (6)$$

Then, while sound radiation of frequency  $\omega$  travels a distance  $c_o T$  during a single period  $T = 2\pi/\omega$ , its source moves a distance  $wT$  nearer to the observer. Thus the wavelength  $\lambda$  (distance between crests) is reduced to

$$\lambda = c_s T - wT = 2\pi(c_s - w)/\omega, \quad (7)$$

and the frequency heard by the observer ( $2\pi$  divided by the time  $\lambda/c_s$  between arrival of crests) is increased to its Doppler-shifted value: the "relative" frequency

$$\omega_r = \omega(1 - w/c_s)^{-1} = \omega[1 - (V/c_s)\cos\theta]^{-1}; \quad (8)$$

though this, of course, may represent a decrease where the angle  $\theta$  is obtuse.

The corresponding change in effective volume results from an effective change in the source's dimension  $\ell$  in the direction of the observer (Lighthill 1962). Because the near side  $N$  of the source region is closer by a distance  $\ell$  than its far side  $F$ , there is a certain "lag"  $\tau$  between the times of emission from  $F$  and  $N$  of sounds that reach the observer simultaneously. Then in the time  $t$  for sound from  $F$  to arrive it travels a distance  $c_s t$ , but the corresponding emission from  $N$  starts after a time lag  $\tau$  during which its distance from  $F$  in the direction of the observer has increased from  $\ell$  to  $\ell + w\tau$ , and the sound emitted then travels a distance  $c_s(t - \tau)$ . The condition for both sounds to reach the same point at time  $t$  may be written

$$c_s t = \ell + w\tau + c_s(t - \tau), \text{ giving } \tau = \ell/(c_s - w). \quad (9)$$

The source's effective dimension in the direction of emission is therefore altered to

$$\ell + w\tau = \ell(1 - w/c_s)^{-1} = \ell\omega_r/\omega; \quad (10)$$

a change by the same Doppler factor  $\omega_r/\omega$  that modifies the frequency. Indeed, the eddy's effective volume during emission is also increased by the Doppler factor  $\omega_r/\omega$ , because dimension in the direction of the observer is so increased whilst other dimensions are unaltered.

Because the effective eddy volume  $\ell^3$  appears to the first power in expression (5), whilst effective frequency occurs to the fourth power in the mean

square of the second time derivative  $\ddot{T}_y$ , these Doppler effects produce an overall modification by five Doppler factors (Ffowcs Williams 1963, Lighthill 1963),

$$(\omega/\omega)^5 = (1 - w/c_o)^{-5} = [1 - (V/c_o)\cos\theta]^{-5}, \quad (11)$$

in the intensity pattern (5) radiated per unit volume of turbulence. This gives a first indication of an important preference for forward emission from turbulence convected at "not so low" Mach number.

On the other hand, it is essential to recognise how, as  $V/c_o$  increases, Doppler effect tends also to degrade the compactness of aeroacoustic sources in relation to forward emission. Not only does  $\omega\ell/c_o$  increase in proportion to Mach number, but an even greater value is taken by  $\omega,\ell/c_o$ , the ratio which must be small if convected sources are to be compact. A very marked restriction on the extent (11) of intensity enhancement for forward emission as  $V/c_o$  increases is placed by these tendencies (Ffowcs Williams 1963, Lighthill 1963, Dowling, Ffowcs Williams & Goldstein 1978). They can develop, indeed, to a point where the compact-source approximation (of low-frequency acoustics) may appropriately be replaced by its opposite (high-frequency) extreme: the ray-acoustics approximation. Thus, for supersonic source convection ( $V/c_o > 1$ ), the relative frequency (8) becomes infinite in the Mach direction

$$\theta = \cos^{-1}(c/V); \quad (12)$$

moreover, it may be shown that radiation from the source proceeds along rays emitted in the Mach direction (Ffowcs Williams & Maidanik 1965).

As this is a paper which devotes special attention to such radiation in the Mach direction, some immediate comments on its nature may perhaps be made. Equation (6) shows that the source's velocity of approach  $w$  towards an observer positioned at an angle (12) to its direction of motion is the sound speed  $c_o$ . On linear theory this means that different parts of a signal are observed simultaneously — which, of course, is the well known condition of stationary phase satisfied on

rays (Lighthill 1978). Sounds emitted by a source approaching at a speed  $w$  exceeding  $c_0$  would be heard by the observer in reverse order (so that "pap pep pip pop pup" became "pup pop pip pep pap"! ) but when  $w = c_0$  all the sounds (vowels and consonants!) would be heard together as one single "boom".

From these preliminary comments the importance of two influences treated in later sections, that place limits on the signal propagated along rays, will already be clear. These are (i) the duration  $\delta$  of well-correlated emission from turbulent eddies and also (ii) nonlinear propagation involving a departure of the signal velocity from  $c_0$ .

## 5. Uniformly valid Doppler-effect approximations

The correlation duration  $\delta$  for convected turbulent eddies is defined so that velocities at times separated by substantially more than  $\delta$  are almost uncorrelated while there is good correlation between velocities at times separated by substantially less than  $\delta$ . This definition in terms of time separations (for the moving eddy) is directly parallel to the definition of  $\ell$  in terms of spatial separations.

Combined use of correlation length  $\ell$  and duration  $\delta$  affords an approximation to the radiation pattern from convected eddies that has some value at all Mach numbers. Thus it is a uniformly valid approximation, spanning the areas of applicability of the compact-source and ray-acoustics approximations.

Figure 1 uses space-time diagrams where the space-coordinate (abscissa) represents distance in the direction of the observer. Diagram (a) for unconvected eddies approximates the region of good correlation, which must have spatial and temporal dimensions  $\ell$  and  $\delta$ , as a simple smooth curve; actually, an ellipse with  $\ell$  and  $\delta$  as its axes. Diagram (b) shows how the region of good correlation is

sheared (sheared, in fact, by a distance  $w$  per unit time) for convected eddies approaching the observer at velocity  $w$ .

Signals from a far point  $F$  and a near point  $N$ , in either case, reach the observer simultaneously — as do signals from other points on the line  $FN$  — provided that this line slopes by a distance  $c_o$  per unit time. Then diagram (b) distinguishes three cases as follows:

- (i) in the compact-source case  $w/c_o$  is small, and the space component of  $FN$  in diagram (b) is  $\ell(1 - w/c_o)^{-1}$ , just as in equation (10) for the "usual" Doppler effect (which neglects the upper bound  $\delta$  on correlation duration);
- (ii) in the ray-acoustics case  $w/c_o \approx 1$ , and the space component of  $FN$  is  $c_o\delta$ ;
- (iii) in the intermediate case  $w/c_o$  is but moderately less than 1, and the space component of  $FN$  is  $\ell$  multiplied by an enhancement factor

$$\left[ (1 - w/c_o)^2 + (w/c_o\delta)^2 \right]^{-1/2}. \quad (13)$$

Evidently, this form (13) of the enhancement factor comprehends all three cases and represents the effective augmentation of source volume due to convection.

The enhancement factor (13) needs to be applied, not only to the volume term  $\ell^3$  in the quadrupole field (5), but also twice to each of the pair of twice-differentiated terms inside the mean square; essentially, because time-differentiations in quadrupole fields arise from differences in the time of emission by different parts of the quadrupole source region — and the time component of  $FN$  in diagram (b) is simply the space component divided by  $c_o$ . As before, then,



five separate factors (13) enhance the intensity field; and, with  $w$  replaced by  $V \cos \Theta$ , expression (11) for the overall intensity modification factor is replaced by

$$\{[1 - (V/c_0) \cos \Theta]^2 + (\ell/c_0 \delta)^2\}^{-3/2}. \quad (14)$$

This is a significant change wherever  $1 - (V/c_0) \cos \Theta$  is relatively small, and it tends to limit the predicted preference for forward emission (Ffowcs Williams 1963, Lighthill 1963).

It also gives an improved description of the influence of Doppler effect on the overall acoustic power output from convected turbulence. For example, the solid line in diagram (c) gives a log-log plot of the average value (spherical mean) of the modification factor (14) as a function of  $V/c_0$  on the reasonable assumption that  $\ell = 0.6 V\delta$ . It will be noted that, as  $V/c_0$  increases, this average modification factor rises a little at first, but falls drastically like  $5(V/c_0)^{-5}$  for  $V/c_0$  significantly greater than 1.

On the other hand aerodynamic noise at low Mach number (see above) has an acoustic efficiency  $\eta$  scaling as  $(U/c_0)^5$  where  $U$  is a characteristic velocity in the flow. Actually, it would be permissible to take that characteristic velocity as the eddy convection velocity  $V$ ; although, if this were done in the case of a jet, it would be important to recognize that  $V$  is not the jet exit speed itself but takes values between 0.5 and 0.6 times the jet exit speed. Thus, an order of magnitude  $10^{-4}(U/c_0)^5$  for  $\eta$  in terms of jet exit velocity  $U$  corresponds to an order of magnitude  $10^{-3}(V/c_0)^5$  in terms of the eddy convection velocity  $V$ .

The broken line in diagram (c) shows how this acoustic efficiency  $\eta$ , supposed to take the value  $10^{-3}(V/c_0)^5$  for small  $V/c_0$ , is modified after multiplication by the average modification factor (solid line). This modification causes  $\eta$  to approach a constant value of about 0.005 (aeroacoustic saturation) at

high Mach numbers, when slightly less than 1% of jet power is radiated as aerodynamic noise.

Supersonic jets are called "properly expanded" when they emerge — from appropriately shaped nozzles — as parallel flows. This is a contrasting case to that of a supersonic jet emerging as a non-parallel flow, which is necessarily followed by a sequence of shock waves (leading to augmentation of aerodynamic noise) in the characteristic "diamond" shock-cell pattern.

Aeroacoustic saturation similar to that indicated in diagram (c) is observed for properly expanded supersonic jets, with acoustic efficiency becoming close to an asymptotically constant value of a little less than  $10^{-2}$  when the jet Mach number  $U/c_0$  exceeds about 2. These are the "extreme-speed" jets, with  $V$  itself (the eddy convection velocity) exceeding  $c_0$ , for which aerodynamic noise is directed (Ffowcs Williams and Maidanik 1965) along rays inclined at the Mach angle (12). Before dedicating the remainder of the lecture to the nature of aerodynamic noise in this extreme-speed limit, I have attempted through the above discussion to exhibit that continuous trend of changing noise patterns which links it to the problem of aerodynamic noise at low Mach number.

## 6. Nonlinear propagation of noise from extreme-speed jets

Extreme-speed jets have just been defined as those properly expanded jets, with speeds more than twice the atmospheric sound speed  $c_0$ , for which the eddy convection velocity  $V$  is itself supersonic and noise is primarily emitted in the Mach direction (12). Significant influences on this type of aerodynamic noise are exerted, not only by correlation duration (see above) for a supersonically moving eddy, but also by important consequences of nonlinear propagation.

Indeed, in a rather obvious analogy with a supersonically moving body, we may expect each eddy's sound field not only (i) to be emitted in the Mach direction but also (ii) to take the form of a "supersonic boom" which, from nonlinear propagation effects, incorporates one or more shock waves. On the other hand, because it is a chaotic sequence of supersonically moving eddies that generates such waveforms, the jet's near noise field must consist (as is, indeed, observed) of a thickly packed random assemblage of conical shock waves.

Thus although, as just remarked, there may be some sort of continuous trend in the mechanisms of generation of aerodynamic noise between classical processes at lower Mach numbers and such extreme-speed jets, nevertheless studies of its propagation become quite different in this latter case. As a marked contrast to approaches that use the full nonlinear flow equations in the jet and simple linear equations of propagation outside it (generation being associated with differences between the equations), it becomes necessary to recognize important nonlinear effects on propagation itself.

In the literature of aerodynamic noise for extreme-speed jets there already exist studies of the generation process that go far beyond the perfunctory sketches which I have included in this lecture. On the other hand, a properly detailed investigation of nonlinear effects on its propagation appears to have been neglected. For this reason, I have chosen to devote the rest of this lecture to such a detailed study of the nonlinear propagation of a thickly packed assemblage of conical shock waves once it has been formed.

Briefly, this detailed study demonstrates how the inherent tendency of the shock strengths to decay (through conical spreading and internal dissipation) is counteracted in part by increases in strength that occur whenever adjacent shocks unite. A certain "bunching" tends to arise, because union of two adjacent shocks is found to increase the likelihood of further union with other neighbouring shocks.

The high-frequency part of the noise spectrum is made more intense than it would otherwise be by these bunching tendencies.

A well known transformation of coordinates (Lighthill 1978) — suggested by the above-noted analogy with supersonic-boom theory (Whitham 1956) — is used (see Appendix) to reduce the problem of conical propagation, aimed at analysing how a temporal waveform varies with distance  $r$  along the Mach direction, to a plane-wave problem. In this latter problem the time  $t$  replaces  $r^{1/2}$ , and attention is focussed on how a given spatial waveform varies with time.

The spatial waveform assumed in this latter context is however immensely more complicated than the simple "N-wave" form appearing in supersonic-boom theory. Instead, it is a spatially unlimited assemblage of random sawtooth waves of the type into which a general plane sound wave of large amplitude would evolve during a certain time  $t$ .

This assemblage comprises randomly located shocks (with random strengths) separated by expansion waves in which the slope of the quantity "excess signal velocity" (excess, that is, over the undisturbed sound speed  $c_0$ ) as a function of position takes the value  $1/t$ . The inherent tendency of the shocks themselves is also to decay like  $1/t$ ; but, as already described, this tendency is opposed whenever shocks unite with adjacent shocks.

After an inverse transformation into the original variables describing conical propagation,  $t$  is replaced by  $r^{1/2}$  but predicted shock strengths have to be divided by a further  $r^{1/2}$  factor. Thus the basic tendency of the shock strengths is now to decay like  $1/r$ ; but, yet again, the opposing tendency described above as "bunching" may prove to be important for the analysis of how aspects of aerodynamic noise are modified in the region of conical propagation that surrounds an extreme-speed jet.

## 7. Random sawtooth waves in transformed coordinates

The classical transformation described in the Appendix addresses the problem of how a thickly packed random assemblage of conical shock waves will evolve with increasing  $r$  (distance in the direction of propagation) by reducing it to an interesting, yet hitherto neglected, problem of plane-wave propagation. This plane-wave problem, which will now be defined, treats the evolution in time of a spatially unlimited assemblage of random sawtooth waves.

Because a random sawtooth wave is primarily important as a form of acoustic noise, any useful specification of such a wave must be one which facilitates identification of its noise spectrum. Now, noise spectra are determined in practice — whether in a physical or in a numerical experiment — from signal records of very great yet finite length which are Fourier analysed by F.F.T. techniques.

Moreover any such Fourier analysis of a signal in an interval of great yet finite length expresses it essentially as a Fourier series, where successive terms in the series describe oscillations with very closely neighbouring frequencies. The noise spectrum is proportional to the squares of their amplitudes, regarded as a function of frequency, and the very close spacing between neighbouring frequencies allows it in practice to be depicted as a continuous curve.

Actually, the Fourier series in question represents an exactly periodic function, with period equal to the length of the interval. Specifically, it represents the unique periodic function (with that period) which coincides with the signal record within the interval.

These considerations lead us, in any study of spatially unlimited waves of random sawtooth type, to focus attention in practice on a random sawtooth wave which is specified on an interval of great but finite length  $L$ ; while, for

completeness, its form outside that interval is defined by requiring it to be a periodic function with period  $L$ . There is no implication here that our interest is really confined to strictly periodic functions; on the contrary, we are interested in waves that, besides being spatially unlimited, have an everywhere random character. But we recognize that any physical or numerical experiment will confine attention to an interval of great but finite length  $L$  within which Fourier analysis of the signal gives a representation of it as an exactly periodic function of period  $L$ , and it is this representation which we find fruitful to analyse.

Plane waves travelling in the  $x$ -direction in a homogeneous medium with undisturbed sound speed  $c_0$  may in nonlinear acoustics be conveniently described in terms of an independent variable

$$X = x - c_0 t \quad (15)$$

and a dependent variable equal to the excess signal velocity

$$v = u + c - c_0, \quad (16)$$

where  $u$  is the fluid velocity and  $c$  the local sound speed (equal to  $c_0 + 0.2u$  in air). In a frame of reference moving at speed  $c_0$ , as defined by the space coordinate  $X$ , any value of  $v$  is propagated at a velocity equal to  $v$  itself.

This is the result which, whenever  $v$  is continuous, may be represented by the familiar partial differential equation

$$\partial v / \partial t + v \partial v / \partial X = 0, \quad (17)$$

with its characteristics of slope  $v$  in the  $(t, X)$  plane. However, the system necessarily tends to develop shocks, which will here be treated as discontinuities. The speed of a shock is equal to the average of the smaller and greater values of  $v$  which appear ahead of and behind it; accordingly, the shock absorbs characteristics ahead of it by running into them, while absorbing characteristics from behind as they run into it.

It may be shown (for example, by differentiating (17) with respect to  $X$ ) that the reciprocal slope  $(\partial v / \partial X)^{-1}$  of continuous parts of the wave must increase at unit rate along any characteristic. It means that any negative value of the reciprocal slope must after a finite time increase to zero, corresponding to infinite slope. This, of course, is when a shock appears, with its subsequent propagation governed by laws quoted above.

By contrast, any positive initial value of the reciprocal slope must grow indefinitely at unit rate, which after a time  $t$  adds a term  $t$  to that initial value. When  $t$  has become large, this added term  $t$  has become dominant over the initial value (at least, if this is not too big), so that to a close approximation the slope  $\partial v / \partial X$  itself takes the value  $1/t$ . Indeed, a classically familiar argument why this must prove to be rather a good approximation is that, when  $t$  has become large, all characteristics with relatively bigger initial values of the reciprocal slope have disappeared through running into shocks; essentially, because of their tendency to be close to characteristics with negative initial values of reciprocal slope (from which shocks necessarily develop). The continuous parts of the waveform are dominated, therefore, by characteristics on which the slope has become close to  $1/t$ .

These are the reasons why an initial random acoustic wave of large amplitude develops after time  $t$  into what we define as a random sawtooth wave. This comprises shocks at positions

$$X = X_n \quad (-\infty < n < \infty) \quad (18)$$

with  $X_n$  a decreasing function of the integer  $n$ ; where the values of  $v$  behind and ahead of the  $n$ th shock are

$$v_n \quad \text{and} \quad v_n - z_n, \quad (19)$$

and where we shall describe as the "strength" of the  $n$ th shock the discontinuity  $z_n$  between the values of  $v$  behind and ahead of it. Moreover, the distribution of  $v$

has the slope  $1/t$  between shocks, so that the value  $v_n - z_n$  of  $v$  just ahead of the  $n$ th shock is related to its value  $v_{n-1}$  just behind the  $(n - 1)$ th shock by the equation

$$v_n - z_n = v_{n-1} - (X_{n-1} - X_n)/t. \quad (20)$$

The decision to assume the wave periodic with period  $L$ , which has already been carefully explained, has certain consequences for the quantities (18) and (19). At any particular time  $t$  there will be a certain specific number  $N$  of shocks within a single period; here,  $N$  is a function of the time, taking integer values, which is reduced discontinuously by 1 at every instant when a union of two shocks occurs. The periodicity then implies that

$$v_{n+N} = v_n, \quad z_{n+N} = z_n, \quad X_{n+N} = X_n - L; \quad (21)$$

so that equation (20), summed between  $n = 1$  and  $n = N$ , gives

$$\sum_{n=1}^N z_n = Lt. \quad (22)$$

This equation, indicating a balance between the net compressive and expansive effects in the sawtooth wave, ensures that the period  $L$  remains unchanged because the sum of the shock strengths on the left-hand side is found (see below) to vary as  $1/t$ .

Figure 2 illustrates the form of a random sawtooth wave at a particular time  $t = T$ , with the number  $N$  of shocks inside the period  $0 < X < L$  equal to 25. The randomness of this wave derives from the fact that a random number generator was used to determine all the strengths  $z_n$  of the 25 shocks and all the spacings  $h_n = X_{n-1} - X_n$  between shocks, subject to

- (i) the need, which equation (21) demonstrates, for the sum of the spacings  $h_n$  to be  $L$ ;
- (ii) the corresponding condition (22) on the sum of the strengths; and
- (iii) restrictions on each value of  $h_n$  or of  $tz_n$  to lie between  $0.01L$  and  $0.09L$ .



Thus the spacings and strengths, subject to (i) and (ii), take random values between these upper and lower bounds. (Here, while the upper bound is intended to reflect some sort of limitation on sizes and strengths of noise sources, the lower bound is imposed mainly for convenience of graphical representation.) The above values fix uniquely a plot of  $v$  against  $X$  with zero integral over a period, and the evolution of this particular sawtooth wave is exhibited in section 11 below.

For a random function  $v$  of  $X$  defined in an interval  $0 < X < L$  (here, a particular single period for the function), its noise spectrum as defined so that  $P(k)dk$  represents the contribution to the function's mean square from wavenumbers between  $k$  and  $k + dk$  is classically given as

$$P(k) = \frac{1}{\pi L} \left\langle \left| \int_0^L v e^{-ikx} dx \right|^2 \right\rangle \quad (23)$$

where the angle brackets denote a statistical mean value. The high-wavenumber behaviour of this noise spectrum, for a random sawtooth function  $v$  dominated by discontinuous changes  $z_n$  at points  $X_n$  as in (18) and (19), is

$$P(k) = \frac{1}{k^2 \pi L} \left\langle \left( \sum_{n=1}^N z_n e^{-ikX_n} \right) \left( \sum_{n=1}^N z_n e^{ikX_n} \right) \right\rangle = \frac{1}{k^2 \pi L} \sum_{n=1}^N z_n^2, \quad (24)$$

so that it depends on the sum of the squares of the shock strengths  $z_n$ .

It is this dependence which makes unions of shocks important. At any such union, the sum of the shock strengths themselves remains unchanged; however, the sum of their squares is necessarily increased, so that the high-frequency part of the noise spectrum is intensified.

## 8. Sawtooth-wave evolution up to when a first union occurs

The dynamics of the shocks is analysed next up to when a union first occurs. At each instant the basic law

$$\dot{X}_n = v_n - \frac{1}{2}z_n, \quad (25)$$

which expresses the velocity  $X_n$  of a shock wave as the average of the values (19) of  $v$  behind and ahead of it, implies also that

$$\dot{v}_n = -(\frac{1}{2}z_n)/t \quad (26)$$

because, during a small time  $\delta t$ , the shock absorbs into itself from behind a section  $\frac{1}{2}z_n \delta t$  of smooth waveform with slope  $1/t$ .

Now careful study of the system of equations (25), (26) and (20) shows that their completely general solution takes the form

$$tz_n = Y_n, \quad v_n = b_n + (Y_n/2t), \quad X_n = a_n + \frac{1}{2}Y_n + b_n t, \quad (27)$$

where  $a_n$ ,  $b_n$  and  $Y_n$  are constants satisfying

$$a_{n-1} - a_n = Y_n. \quad (28)$$

This solution gives a constant value  $Y_n$  to the product of the shock strength  $z_n$  with the time  $t$ . Here, as noted earlier,  $t$  is measured from an origin ( $t = 0$ ) when the waveform was initiated, so that it later developed into a sawtooth wave with the slope  $1/t$  for all smooth sections thereof.

Great interest attaches to the distance  $h_n = X_{n-1} - X_n$  between two adjacent shocks. Equations (27) and (28) show that

$$h_n = \frac{1}{2}(Y_{n-1} + Y_n) + (b_{n-1} - b_n)t. \quad (29)$$

Now, as noted earlier, the analysis in this lecture is only concerned with propagation of random sawtooth waves once they have appeared; say, from  $t = T$  when  $h_n$  takes the form

$$H_n = \frac{1}{2}(Y_{n-1} + Y_n) + (b_{n-1} - b_n)T. \quad (30)$$

Eliminating the unknown constant  $b_{n-1} - b_n$  between (29) and (30) we obtain an equation for the evolution of  $h_n$  in the form

$$h_n = (t/T)[H_n - (Y_{n-1} + Y_n)\sigma], \quad (31)$$

where it proves useful to introduce a new time-like variable  $\sigma$ . The equations

$$\sigma = (t - T)/2t, \quad t = T/(1 - 2\sigma) \quad (32)$$

make  $\sigma$  an increasing function of  $t$  and map the unbounded interval  $T < t < \infty$  into the finite interval  $0 < \sigma < 1/2$ . It turns out that  $\sigma$  is a highly convenient measure of the times at which unions of shocks occur.

As just a preliminary example of this, we note from equation (31) that the very first union of two shocks occurs when

$$\sigma = \text{Min}_{1 \leq n \leq N} [H_n / (Y_{n-1} + Y_n)], \quad (33)$$

since it is this value of  $\sigma$  that first allows one of the  $h_n$  (distances between shocks) to fall to zero. Because of the periodicity assumption which was exhaustively discussed earlier, the minimum (33) must of course be attained not only for a particular value  $n$  within the period  $1 \leq n \leq N$  but also for the corresponding value  $(n \pm mN)$ , with  $m$  an integer) in any other period. Attention is here focussed, however, on a single period — except for the fact that when equation (28) or (33), or any other equation involving  $n - 1$ , is applied to (say)  $n = 1$ , periodicity is used to interpret  $n - 1$  as  $N$ .

On the other hand, there is no need in a random sawtooth wave to consider the possibility (really an impossibility — since it would occur with zero measure in a probability space of random variables) that the same minimum value (33) might be attained for two different  $n$  in the period  $1 \leq n \leq N$ . It will be assumed

rather that the first union occurs for a particular  $n$  and  $\sigma$ , as specified by equation (33). Also, because equations (22) and (27) imply that

$$\sum_{n=1}^N Y_n = L = \sum_{n=1}^N H_n \quad (34)$$

the minimum (33) is readily shown to satisfy the requirement,  $\sigma < 1/2$ , for it to correspond to an actual time  $t > T$  for first union between shocks.

Until this time, of course, every  $Y_n$  (defined as the product of the strength of the  $n$ th shock with the time  $t$ ) has remained constant. Then a first union — say, of the  $n$ th and  $(n - 1)$ th shocks — produces addition of their strengths  $z_n$  and  $z_{n-1}$ , with consequences noted earlier for the high-frequency form (24) of the noise spectrum.

In the meantime, there is a reduction by 1 in the number  $N$  of shocks in a single period, but the sum on the left-hand side of (34) continues to take the value  $L$  simply because the new shock, replacing those associated with the  $Y$ -values  $Y_n$  and  $Y_{n-1}$ , takes on their added  $Y$ -value  $Y_n + Y_{n-1}$ . Similarly equation (34) remains unchanged at all later unions — other properties of which will now be investigated.

## 9. Formulas specifying all later unions of shocks

In this section, the tendency to "bunching" of shocks — that is, an increased likelihood of union between shocks that have already participated in union with other shocks — is quantified by means of a general formula for the time of union of two shocks which allows for all preceding unions. The two shocks to be considered are taken as (i) a shock originally numbered  $n$ , into which other shocks have merged from behind, and (ii) a shock originally number  $n - 1$ , which has run into (and merged with) various shocks ahead of it.

Evidently, this is the most general possible merger. Indeed, when any pair of shocks unite, it is permissible to "identify" the back one with an original shock (numbered  $n$ , say) into which others have merged from behind, and the front one with an original shock (numbered  $n - 1$ , say) that has run into others ahead of it.

Specifically, we shall suppose that the shock originally numbered  $n$  has participated in a total number  $m_n$  of unions with shocks from behind, with  $Y$ -values

$$Y_{Bm}, \text{ occurring at times } t = t_{Bm} (m = 1 \text{ to } m_n). \quad (35)$$

Similarly, we assume that the shock originally numbered  $n - 1$  has participated in a total number  $m_{n-1}$  of unions with shocks ahead of it, with  $Y$ -values

$$Y_{Am}, \text{ occurring at times } t = t_{Am} (m = 1 \text{ to } m_{n-1}). \quad (36)$$

It is convenient to embark upon this problem by considering first the dynamics of the shock originally numbered  $n$  immediately after it has undergone just the first of the above unions, at  $t = t_{B1}$ . Because we "identify" this merged shock with the shock originally numbered  $n$ , we continue to use the subscript  $n$  in quantities such as (18) and (19) associated with this shock. Then the differential equations (25) and (26) continue to apply to this united shock, as does the relationship (20), so that the form (27) of this system's general solution is unaltered. However, the constants  $a_n$ ,  $b_n$  and  $Y_n$  are changed to new values

$$a_n = Y_{B1}, \quad b_n = (Y_{B1}/2t_{B1}), \quad Y_n = Y_{B1}; \quad (37)$$

while (28) is still satisfied since  $a_{n-1}$  has not been changed.

Out of these new values (37) for  $a_n$ ,  $b_n$  and  $Y_n$ , the last (added  $Y$ -values for uniting shocks) has been explained above. Also, we may readily verify that the new values for  $a_n$  and  $b_n$  are the only ones which satisfy two essential conditions: that union at time  $t = t_{B1}$  makes no discontinuous change in the position  $X_n$  of the  $n$ th shock, while increasing  $v_n$  (the value of  $v$  behind it) by  $z_{B1} = Y_{B1}/t_{B1}$  (the merging shock's jump in  $v$ ).

Similar studies show that, in each subsequent union of the  $n$ th shock with shocks from behind as specified in (35), the constants receive further changes as in (37) but with  $Y_{Bm}$  and  $t_{Bm}$  replacing  $Y_{B1}$  and  $t_{B1}$ ; so that, after all of them,  $a_n$ ,  $b_n$  and  $Y_n$  have become

$$a_n = \sum_{m=1}^{m_n} Y_{Bm}, \quad b_n = \sum_{m=1}^{m_n} (Y_{Bm}/2t_{Bm}), \quad Y_n = \sum_{m=1}^{m_n} Y_{Bm}. \quad (38)$$

Other careful studies of the unions of the  $(n-1)$ th shock with shocks ahead of it as specified in (36) demonstrate that, when all are completed,  $a_{n-1}$ ,  $b_{n-1}$  and  $Y_{n-1}$  have become

$$a_{n-1} = \sum_{m=1}^{m_{n-1}} Y_{Am}, \quad b_{n-1} = \sum_{m=1}^{m_{n-1}} (Y_{Am}/2t_{Am}), \quad Y_{n-1} = \sum_{m=1}^{m_{n-1}} Y_{Am}. \quad (39)$$

These results allow both  $X_n$  and  $X_{n-1}$  to be obtained by use of (27), so that the separation  $h_n = X_{n-1} - X_n$  between the shocks can be expressed as

$$h_n = \frac{1}{2}(Y_{n-1} + Y_n) + (b_{n-1} - b_n)t - \frac{1}{2} \sum_{m=1}^{m_{n-1}} Y_{Am}(t/t_{Am} - 1) - \frac{1}{2} \sum_{m=1}^{m_n} Y_{Bm}(t/t_{Bm} - 1). \quad (40)$$

Here, equation (30) may be used to substitute for  $b_{n-1} - b_n$  in terms of the value  $H_n$  of the separation  $h_n$  at the initial time  $t = T$ . Then, with times  $t$ ,  $t_{Am}$  and  $t_{Bm}$  substituted in terms of the corresponding  $\sigma$ -values from (32), we obtain

$$(1 - 2\sigma)h_n = H_n - (Y_{n-1} + Y_n)\sigma - \sum_{m=1}^{m_{n-1}} Y_{Am}(\sigma - \sigma_{Am}) - \sum_{m=1}^{m_n} Y_{Bm}(\sigma - \sigma_{Bm}). \quad (41)$$

Equation (41) gives an elegant and completely general expression for the value of the time-like variable  $\sigma$  when the  $n$ th and  $(n-1)$ th shocks unite (so that  $h_n$  becomes zero). The form of this expression becomes particularly instructive if we use  $\sigma_n$  to signify the ratio

$$\sigma_n = H_n/(Y_{n-1} + Y_n). \quad (42)$$

Equation (31) shows how, provided that  $\sigma_n < 1/2$ , this value of  $\sigma$  specifies the time at which the  $n$ th and  $(n-1)$ th shocks would have united if no other unions of shocks had occurred first.

On the other hand, the actual value of  $\sigma$  corresponding to the time at which the shocks unite is given, by using the substitution (42) after putting  $h_n = 0$  in (41), as

$$\sigma = \frac{(Y_{n-1} + Y_n)\sigma_n + \sum_{m=1}^{n-1} Y_{Am}\sigma_{Am} + \sum_{m=1}^{n-1} Y_{Bm}\sigma_{Bm}}{Y_{n-1} + Y_n + \sum_{m=1}^{n-1} Y_{Am} + \sum_{m=1}^{n-1} Y_{Bm}} . \quad (43)$$

Expression (43) may be recognized as a weighted mean of the  $\sigma$ -values  $\sigma_n$ ,  $\sigma_{Am}$  and  $\sigma_{Bm}$  with weights given in terms of shock strengths according to the following simple rules.

The weight attached to  $\sigma_{Am}$ , or to  $\sigma_{Bm}$ , is  $Y_{Am}$  or  $Y_{Bm}$  respectively; in other words, it is the  $Y$ -value (strength multiplied by  $t$ ) of the shock that merges when  $\sigma = \sigma_{Am}$  with the  $(n - 1)$ th shock or when  $\sigma = \sigma_{Bm}$  with the  $n$ th shock. By contrast, the weight attached to  $\sigma_n$  is the initial combined  $Y$ -values of the  $n$ th and  $(n - 1)$ th shocks which would have united at  $\sigma = \sigma_n$  (provided that  $\sigma_n < 1/2$ , though otherwise not at all) if no preceding unions had occurred. The sum of all these weights, which constitutes the denominator of (43), represents the overall  $Y$ -value of the united shock that results from union of the  $n$ th and  $(n - 1)$ th shocks after they have respectively undergone all the mergers (35) and (36).

## 10. Bunching tendencies and their implications

Very simple properties of the weighted mean (43) tell us that, because all these mergers at the times (35) and (36) have preceded the union of the  $n$ th and  $(n - 1)$ th shocks, so that

$$\sigma > \sigma_{Am} \quad \text{and} \quad \sigma > \sigma_{Bm} \quad \text{for all } m , \quad (44)$$

therefore the quantity  $\sigma_n$ , which is the only other among all the  $\sigma$ -values of which (43) represents the weighted mean, must satisfy the opposite inequality  $\sigma < \sigma_n$ .

In words, the union of the  $n$ th and  $(n - 1)$ th shocks takes place earlier, in consequence of any preceding unions in which either have participated, than would have been the case if no such preceding unions had occurred.

But still more valuable than any such purely qualitative statement is the quantitative expression (43) for the reduced value of  $\sigma$  at the instant of union. For example, in cases when the  $Y$ -values of the  $n$ th and  $(n - 1)$ th shocks were initially rather small — before they merged with stronger shocks — it is of course quite possible for  $\sigma_n$ , as defined by the ratio (42), to be considerably greater than  $1/2$ . This implies that the shocks are initially moving farther apart, so that their union could never have taken place if neither had merged with other shocks. Yet, in the weighted mean (43), the combined weights attached to all the  $\sigma_{Am}$  and  $\sigma_{Bm}$  may greatly exceed that attached to  $\sigma_n$  if the  $Y$ -values of the merging shocks amount in total to much more than the initial combined value  $Y_{n-1} + Y_n$ ; and, evidently, this allows the value (43) for  $\sigma$  (associated with the time of union of the  $n$ th and  $(n - 1)$ th shocks) to be only a little bigger than the greatest of the  $\sigma_{Am}$  and  $\sigma_{Bm}$ .

Such considerations allow us to infer that a random sawtooth wave may be subject to a very marked "bunching" process. This is a process of "snowball" type where early local unions of shocks act to stimulate further unions with neighbouring shocks. Because this process, while leaving the sum of all the  $Y$ -values unchanged, produces an increase in the sum of their squares, it may have an important effect of enhancing (as expression (24) shows) the high-frequency part of the noise spectrum.

## 11. An algorithm facilitating numerical experiments on bunching

Another useful route to the quantitative study of the bunching process is through numerical experiments. In principle, these might be attempted by computing "weak" solutions of equation (17) and scrutinizing their evolution from instant to



instant to identify those times when unions of shocks occur. On the other hand such identifications can be a little inconvenient and somewhat lacking in precision with practical values of the grid spacing.

A much more straightforward approach is one that treats all shocks as discontinuities and which makes use of just a single time-step between each union and the next. The basic result (33), for defining when an initial set of  $N$  shocks within a period  $L$  becomes reduced to a set of  $N - 1$  shocks after the first union of two shocks has occurred, may be applied successively for this purpose in the following algorithmic treatment.

The algorithm starts from  $N$  shocks filling the period  $L$  at a given time  $t$ , with  $Y$ -values  $Y_n$  ( $n = 1$  to  $N$ ) and with spacings  $h_n = X_{n+1} - X_n$  between shocks, where

$$\sum_{n=1}^N h_n = L \text{ and, by (22), } \sum_{n=1}^N Y_n = L. \quad (45)$$

The form of the algorithm is a respecification of all these variables at the instant when the first union of any pair of adjacent shocks has occurred. (This algorithm can then, systematically, be given successive applications to determine subsequent developments, including bunching.)

The most obvious change in one of the variables after that union is that  $N$  has been replaced by  $N - 1$ . All of the other changes, however, depend critically on those quantities which have been shown to define when a union first occurs; namely the minimum (33) and the value of  $n$  for which the minimum is attained.

In the present case we define, then,

$$\sigma_m = \text{Min}_{1 \leq n \leq N} [h_n / (Y_{n-1} + Y_n)], \text{ attained for } n = m, \quad (46)$$

and note that, according to equations (45), this minimum value cannot exceed  $1/2$ . Then the time  $t$  needs to be respecified as the time

$$t/(1 - 2\sigma_m) \quad (47)$$

at which a union first occurs. At that instant the  $m$ th and  $(m - 1)$ th shocks have united, and are designated thereafter as the  $(m - 1)$ th, with  $Y$ -value  $Y_{m-1} + Y_m$ . For other values of  $n$ , the  $n$ th shock retains its  $Y$ -value  $Y_n$ , and is still numbered as the  $n$ th shock for  $n < m - 1$  but now needs to be renumbered as the  $(n - 1)$ th shock for  $n > m$ . Also, equation (31) tells us that the spacing  $h_n$  is changed to

$$[h_n - \sigma_m(Y_{n-1} + Y_n)]/(1 - 2\sigma_m) \quad (48)$$

for  $n \leq m - 1$ . The same change occurs for  $n \geq m + 1$  except that the value of  $n$  is simultaneously replaced by  $n - 1$ .

A special note is required to the effect that quantities involving  $Y_{n-1}$  need when  $n = 1$  to be reinterpreted (by periodicity) with  $Y_{n-1}$  replaced by  $Y_N$ . Similarly, when  $m = 1$ , the united shock is then renumbered as the  $(N - 1)$ th shock, with  $Y$ -value  $Y_N + Y_1$ .

The overall algorithm may be summarised as follows. Given a positive integer  $N$  and a time  $t$ , and a set of intervals and of  $Y$ -values (shock strengths multiplied by the time)  $h_n$  and  $Y_n$  for  $n = 1$  to  $N$ , satisfying equations (45), we determine the minimum (46) where  $Y_0$  is to be interpreted as  $Y_N$ . Then the algorithm

	replaces each of	by the new value
(a)	$N$	$N - 1$
(b)	$t$	$t/(1 - 2\sigma_m)$
(c)	$Y_n$ for $n < m - 1$	$Y_n$
(d)	$Y_{m-1}$ if $m > 1$	$Y_{m-1} + Y_m$
(e)	$Y_{N-1}$ if $m = 1$	$Y_N + Y_1$

- (f)  $Y_n$  for  $m \leq n \leq N - 1$   $Y_{n+1}$   
(unless  $n = N - 1$  and  $m = 1$ )
- (g)  $h_n$  for  $n < m$   $[h_n - \sigma_m(Y_{n-1} + Y_n)]/(1 - 2\sigma_m)$
- (h)  $h_n$  for  $m \leq n \leq N - 1$   $[h_{n+1} - \sigma_m(Y_n + Y_{n+1})]/(1 - 2\sigma_m)$

but it should perhaps be mentioned that, evidently, there are no values of  $n$  for which (c) can be applied if  $m = 1$  or  $2$ , and none for which (f) can be applied if  $m = N$ . Similarly, there are no values of  $n$  for which (g), or else (h), can be applied if  $m = 1$ , or  $m = N$ , respectively. Subject to these interpretations, the algorithm can be very readily executed, and then re-executed as many times as required to determine all subsequent developments of the random sawtooth wave.

Figure 3 shows the results of applying this algorithm to the random sawtooth wave illustrated in Figure 2. That configuration at the initial time  $t = T$ , with its twenty-five shocks, occupies the bottom of the diagram; the rest of which depicts the paths of the shocks, including all unions, for  $T \leq t \leq 7T$ .

During this period there have occurred one bunching of nine shocks, two bunchings of five shocks and one bunching of three shocks; on the other hand, three out of the original twenty-five shocks have avoided participating in any unions. All of this appears consistent with the suggested definition of bunching as a tendency "for shock waves that have already formed unions with other shock waves to acquire an increased proneness to form further unions".

It may be natural to ask whether Figure 3 represents in any sense a "selected" example; this question, however, has a negative answer. Figure 2 was produced, as explained in section 7, by means of a random number generator, and the algorithm of this section was simply applied to the very first wave so generated. I shall be quite content to leave to later investigators the pleasure of

executing all those numerous "runs" of the algorithm that may be necessary to establish statistical trends!

At each and every union, as already mentioned, the sum of the  $Y_n$  remains constant but the sum of their squares increases discontinuously. Figure 4 shows this process in the case of the sawtooth waveform evolution illustrated in Figure 3. Within the interval  $T \leq t \leq 7T$  quite a pronounced rise in  $\Sigma Y_n^2$  is found, and it is intriguing that this discontinuously increasing dependence on  $t$  deviates only a little from a straight line through the origin, which would represent a simple proportionality to  $t$ .

The implication here is that, although the inherent tendency of each shock strength  $z_n = \Delta_n r^{-1}$  is to vary as  $r^{-1}$ , nevertheless the sum  $\Sigma z_n^2$  which appears in the high-frequency noise spectrum (24) shows a variation very different from  $r^{-2}$  and, indeed, one rather close to  $r^{-1}$ . The bunching process, in short, significantly enhances the high-frequency part of the noise spectrum.

## 12. Conclusion

This has been a Lecture which, in the words of its title, has aimed at exploring just "some aspects" of jet noise fields. Indeed, even that single aspect which has been covered in most detail — the nonlinear propagation of the noise signal from extreme-speed jets — has been investigated only in a noise field quite close to the jet, where a rather consistently conical propagation of noise is to be found. This noise has its origin in the jet mixing region, separating an internal core flow of velocity  $U$  from the outside atmosphere, with eddies in this region convected at an approximately constant velocity  $V$  which defines the Mach direction (12) for noise emission.

On the other hand, there exists only a finite length of jet mixing region, beyond which the core flow vanishes and eddy convection velocities immediately

start to fall off with distance. The beam of truly conical noise propagation, then, is only of finite width and, accordingly, can maintain its conical character for only a limited distance from the jet axis. Beyond that distance the propagation must change progressively to a propagation which — although still directional — is beginning to exhibit an essentially spherical attenuation.

Nonetheless, although conscious of all this, I have here placed emphasis on the field of conical noise propagation rather close to the jet for two main reasons. The first applies if our concern really is with just an isolated jet radiating into still air.

Then general nonlinear acoustics (Lighthill 1978) tells us that waveform modifications due to nonlinear propagation effects are enormously greater in a conically spreading wave than in a spherically spreading wave; specifically, the square-root transformation (A4) derived in the Appendix below is replaced by a logarithmic transformation for a spherical wave which, accordingly, undergoes far less modification from nonlinear propagation. The conical field is specially important, then, as the region of occurrence of most of the spectrum-modification effects of nonlinear propagation.

But theoretical studies may have even more importance for the problem of how aero-engine installations are to be designed so as to reduce ground levels. In this context a jet noise field where propagation is directionally concentrated (say, in the Mach direction) may offer engine-installation designers a rather special opportunity to incorporate shielding devices aimed at limiting community noise. This, then, is yet another good reason why, in this inaugural Theodorsen Lecture, I have presented to my distinguished audience quite a detailed analysis of how the noise spectrum in that conical field with its "random assemblage of shocks" may be influenced by the general tendency on which I have affectionately ventured to bestow the name "bunching".

## Appendix. Conical-wave problem transformed into plane-wave case

A classical transformation converts the problem of conically propagating waves incorporating relatively weak shocks into a plane-wave problem. The transformation is effective in any region which for linear acoustics would be described as a far field, with amplitudes varying as  $r^{-1/2}$  along linearised characteristics.

The corresponding law for nonlinear acoustics, in continuous parts of the field, is that amplitudes vary as  $r^{-1/2}$  along characteristics as defined for the nonlinear problem (Whitham 1956). In both cases  $r$  represents propagation distance measured from a zero on the axis of the cones, but a certain lower limit for  $r$  exists beyond which this far-field representation can be applied.

In the conical-wave problem treated here, it may be convenient to use a notation  $t_c$  to signify the time, to avoid confusion with the use of  $t$  as the time for the plane-wave problem, treated above, into which the conical-propagation problem will be transformed. Moreover a suitable dependent variable (also designated by subscript  $c$ ) will be the defect in reciprocal signal velocity (Lighthill 1978),

$$v_c = c_0^{-1} - (u + c)^{-1}, \quad (\text{A1})$$

rather than the excess (16) in the signal velocity itself.

Now the condition that this dependent variable varies as  $r^{-1/2}$  along characteristics satisfying

$$dt_c = (u + c)^{-1} dr = (c_0^{-1} - v_c) dr \quad (\text{A2})$$

may be written

$$\left\{ \partial/\partial r + (c_0^{-1} - v_c) \partial/\partial t_c \right\} (r^{1/2} v_c) = 0. \quad (\text{A3})$$

Then a simple transformation of coordinates

$$2r^{1/2} = t, \quad c_0^{-1} r - t_c = X \quad (\text{A4})$$

transforms the operator in braces into

$$r^{-1/2} \partial/\partial t + c_s^{-1} \partial/\partial X - (c_s^{-1} - v_c) \partial/\partial X ; \quad (\text{A5})$$

so that, if the dependent variable is changed also to  $v = r^{1/2} v_c$ , the equation for  $v$  becomes

$$(\partial/\partial t + v \partial/\partial X) v = 0 , \quad (\text{A6})$$

exactly as in equation (17) above.

It follows that all the results for the plane-wave case can be directly applied to the conical-wave problem, with  $v$  standing for  $r^{1/2} v_c$  and  $t$  for  $2r^{1/2}$ . The temporal evolution (as  $t$  increases) of the spatially unlimited waveform (in  $-\infty < X < \infty$ ) for plane waves is then seen, according to (A4), as a representation of the spatial evolution (as  $r$  increases) of the temporally unlimited waveform (in  $-\infty < t_c < \infty$ ) for conical waves.

In this representation the important quantity  $Y_n$ , which remains constant for each shock until it unites with another shock (when their  $Y$ -values add), stands for the product of  $t$  with the change  $\Delta v$  between the values of  $v$  ahead of and behind the shock. Its corresponding meaning for conical propagation is therefore  $2r\Delta v_c$ , where  $\Delta v_c$  is the shock strength  $z_n$ . Accordingly, in a conically propagating random sawtooth wave, the inherent tendency of shock strengths (while their  $Y$ -values remain constant) is to decay like the reciprocal  $r^{-1}$  of the propagation distance  $r$  from the axis of the cones, although this tendency is opposed wherever shocks unite (through their  $Y$ -values adding).

In the meantime the second of equations (A4) implies that the quantity  $h_n$ , which in the plane-wave case stands for the distance between adjacent shocks at a given time, represents in the conical-wave problem the interval between times of passage of adjacent shocks past a given position with a specified value of  $r$ . Also the quantity  $T$ , used above to signify the time when a plane wave of random sawtooth type can be considered established, must in the conical-wave problem be given the value  $2R^{1/2}$ , where  $R$  stands for the corresponding propagation distance from the axis at which such a wave has become established.

Calculations of times for unions of shocks in the plane-wave case treated above are expressed in terms of a nondimensional variable  $\sigma$ , whose defining equations (32) correspond for conical propagation to the equations

$$\sigma = (r^{1/2} - R^{1/2})/2r^{1/2}, \quad r = R/(1 - 2\sigma)^2. \quad (\text{A7})$$

Expressions for the values of  $\sigma$  at which shocks unite, like (33) for the first such union or (43) for a quite general subsequent union — as given in terms of the  $Y$ -values of shocks and the initial values  $H_n$  of  $h_n$  (now the initial time intervals between shocks) — can then immediately be interpreted, by (A7), as specifying the distance  $r$  required for merger of adjacent shocks. This in turn can be used to quantify tendencies to bunching in conical-wave propagation.

Finally, if numerical experiments like that of section 11 indicate a general tendency for  $\Sigma Y_n^2$  to increase in approximate proportionality to  $t = 2r^{1/2}$ , this has implications for the quantity

$$\sum_{n=1}^N z_n^2 = \sum_{n=1}^N (Y_n/2r)^2 \quad (\text{A8})$$

which equation (24) associates with the high-frequency part of the noise spectrum. Although the inherent tendency of  $z_n$  to decay at  $r^{-1}$  would cause this sum (A8) to vary as  $r^{-2}$ , bunching tendencies modify this decay law for high-frequency noise into a variation as  $r^{3/2}$ .

### Acknowledgment

I am warmly grateful to Professor D.G. Crighton for many helpful comments on the material in this paper.

### References

- Crighton, D.G. 1975 Basic principles of aerodynamic noise generation. *Prog. Aerospace Sci.* **16**, 31-96.



- Curle, N. 1955 The influence of solid boundaries on aerodynamic sound. *Proc. Roy. Soc. A*, **231**, 505-514.
- Dowling, A.P., Ffowcs Williams, J.E. and Goldstein, M.E. 1978 Sound production in a moving stream. *Phil. Trans. Roy. Soc. A*, **288**, 321-348.
- Ffowcs Williams, J.E. 1963 The noise from turbulence convected at high speed. *Phil. Trans. Roy. Soc. A*, **255**, 469-503.
- Ffowcs Williams, J.E. and Hawkings, D.L. 1969 Sound generation by turbulence and surfaces in arbitrary motion. *Phil. Trans. Roy. Soc. A*, **264**, 321-342.
- Ffowcs Williams, J.E. and Maidanik, G. 1965 The Mach wave field radiated by supersonic turbulent shear flows. *J. Fluid Mech.* **21**, 641-657.
- Goldstein, S. 1946 Low drag and suction aerofoils. The Wright Brothers Lecture. *J. Aero. Sci.* **15**, 189-220.
- Hussaini, M.Y. and Hardin, J.C. (eds.) 1993 *Proceedings of the ICASE/NASA La RC Workshop on Computational Aeroacoustics*. National Aeronautics and Space Administration.
- Lassiter, L.W. and Hubbard, H.H. 1952 Experimental studies of noise from subsonic jets in still air. *NACA Tech. Note 2757*. National Advisory Committee for Aeronautics.
- Lighthill, M.J. 1952 On sound generated aerodynamically. I. General theory. *Proc. Roy. Soc. A*, **211**, 564-587.
- Lighthill, M.J. 1954 On sound generated aerodynamically. II. Turbulence as a source of sound. *Proc. Roy. Soc. A*, **222**, 1-32.
- Lighthill, M.J. 1962 Sound generated aerodynamically. The Bakerian Lecture. *Proc. Roy. Soc. A*, **267**, 147-182.
- Lighthill, M.J. 1963 Jet Noise. The Wright Brothers Lecture. *AIAA Journal*, **1**, 1507-1517.
- Lighthill, J. 1978 *Waves in Fluids*. Cambridge University Press.
- Whitham, G.B. 1956 On the propagation of weak shock waves. *J. Fluid Mech.* **1**, 290-318.

## Figure Captions

**Figure 1. A uniformly valid Doppler-effect approximation.**

Diagram (a). Space-time diagram for unconvected "eddies" of correlation length  $\ell$  and duration  $\delta$ .

Diagram (b). Case of "eddies" convected towards observer at velocity  $w = V \cos \Theta$ , being Diagram (a) sheared by a distance  $w$  per unit time. Here, straight lines sloping by a distance  $c_o$  per unit time represent emissions received simultaneously by the observer.

Case (i):  $w/c_o$  small. Case (ii):  $w/c_o = 1$ . Case (iii): intermediate value of  $w/c_o$ .

Diagram (c). Solid line: average (spherical mean) of the modification factor (13). Broken line: acoustic efficiency,  $\eta$ , obtained by applying this factor to a low-Mach-number "quadrupole" efficiency of (say)  $10^{-3}(V/c_o)^5$ .

Application to jets. For a jet of exit speed  $U$ , a typical eddy convection velocity  $V$  takes values between  $0.5U$  and  $0.6U$ . In order of magnitude terms, then, the efficiency  $\eta$  makes a transition, at about  $U/c_o = 2$ , between values around  $10^{-4}(U/c_o)^5$  and an asymptotically constant value of a little less than  $10^{-2}$ .

**Figure 2. A random sawtooth wave, with the number  $N$  of shocks inside the period  $0 < X < L$  equal to 25; and with their spacings and strengths determined, subject to conditions (i), (ii) and (iii), by a random number generator.**

**Figure 3. Results of applying the algorithm of section 11 to the initial waveform of Figure 2. This is reproduced at the bottom of the diagram; the rest of which depicts (by plots of  $X/L$  against  $t/T$ ) the paths of the shocks, including all unions, for  $T \leq t \leq 7T$ . Reading from left to right, note two bunchings of five shocks each, one of three shocks and one of nine shocks, interspersed with three shocks that have avoided participating in any unions.**

Figure 4. A plot of  $\sum_{n=1}^N (Y_n/L)^2$  against  $t/T$ , for the sawtooth waveform evolution illustrated in Figure 3, is used to indicate how bunching enhances the high-frequency part of the noise spectrum.

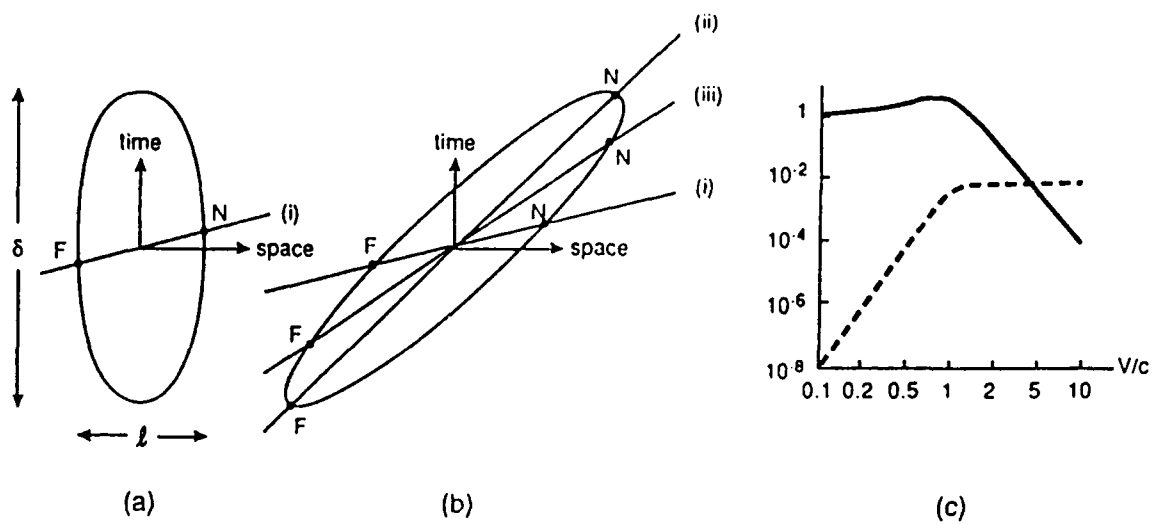


Figure 1.

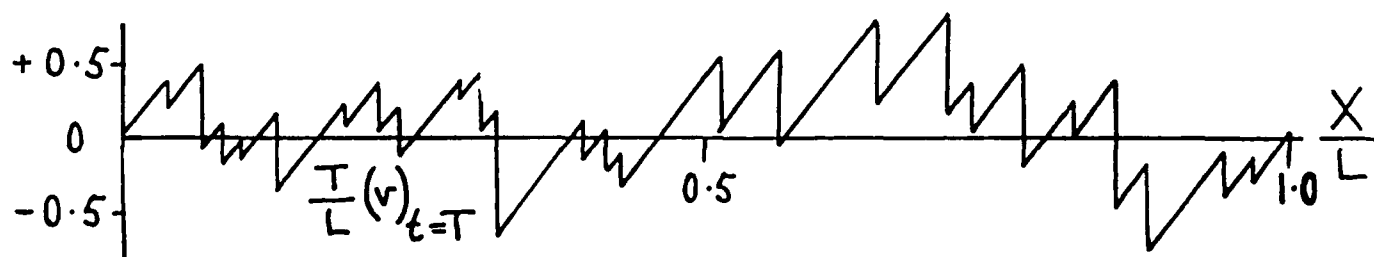


Figure 2.

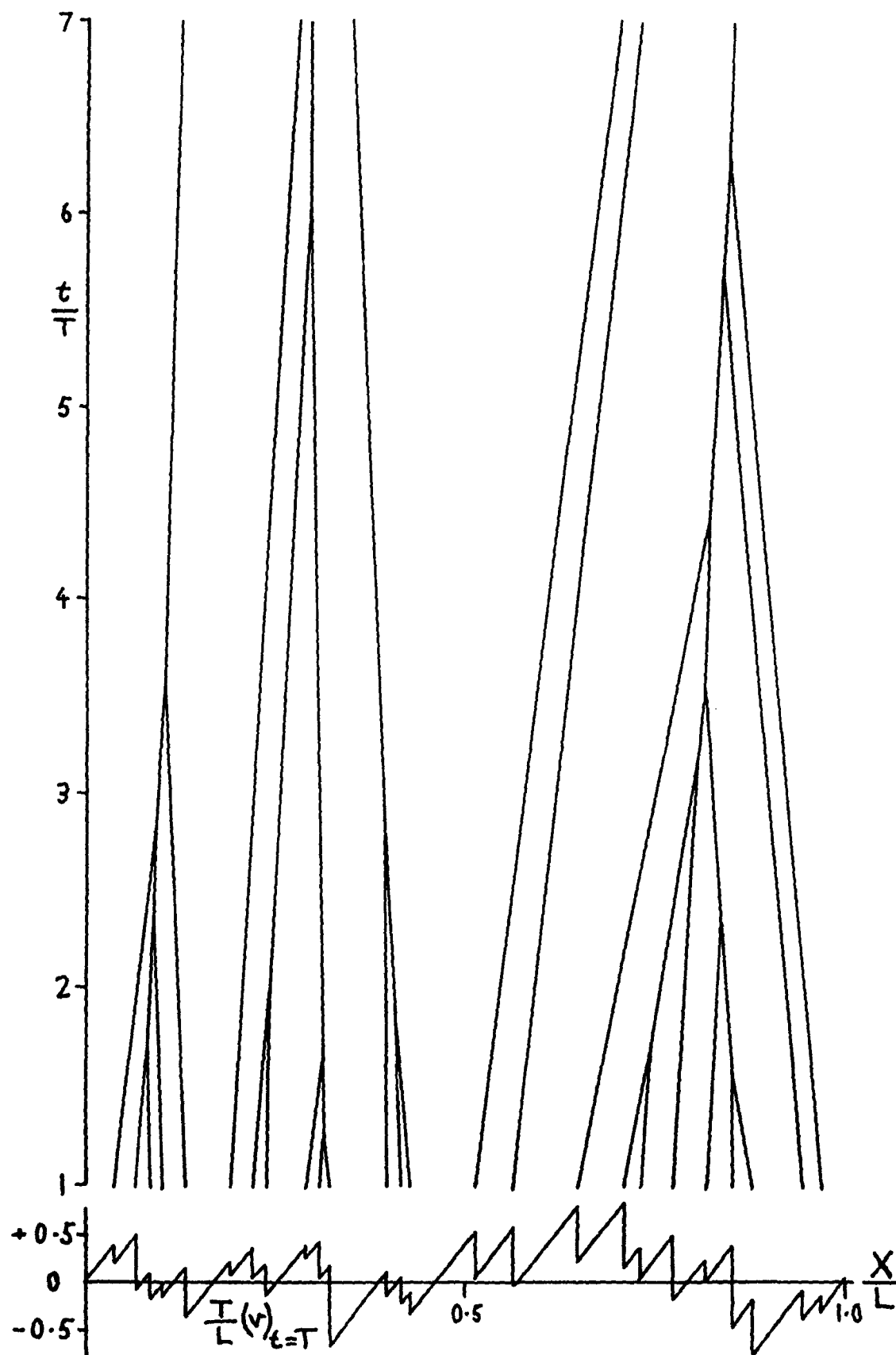


Figure 3.

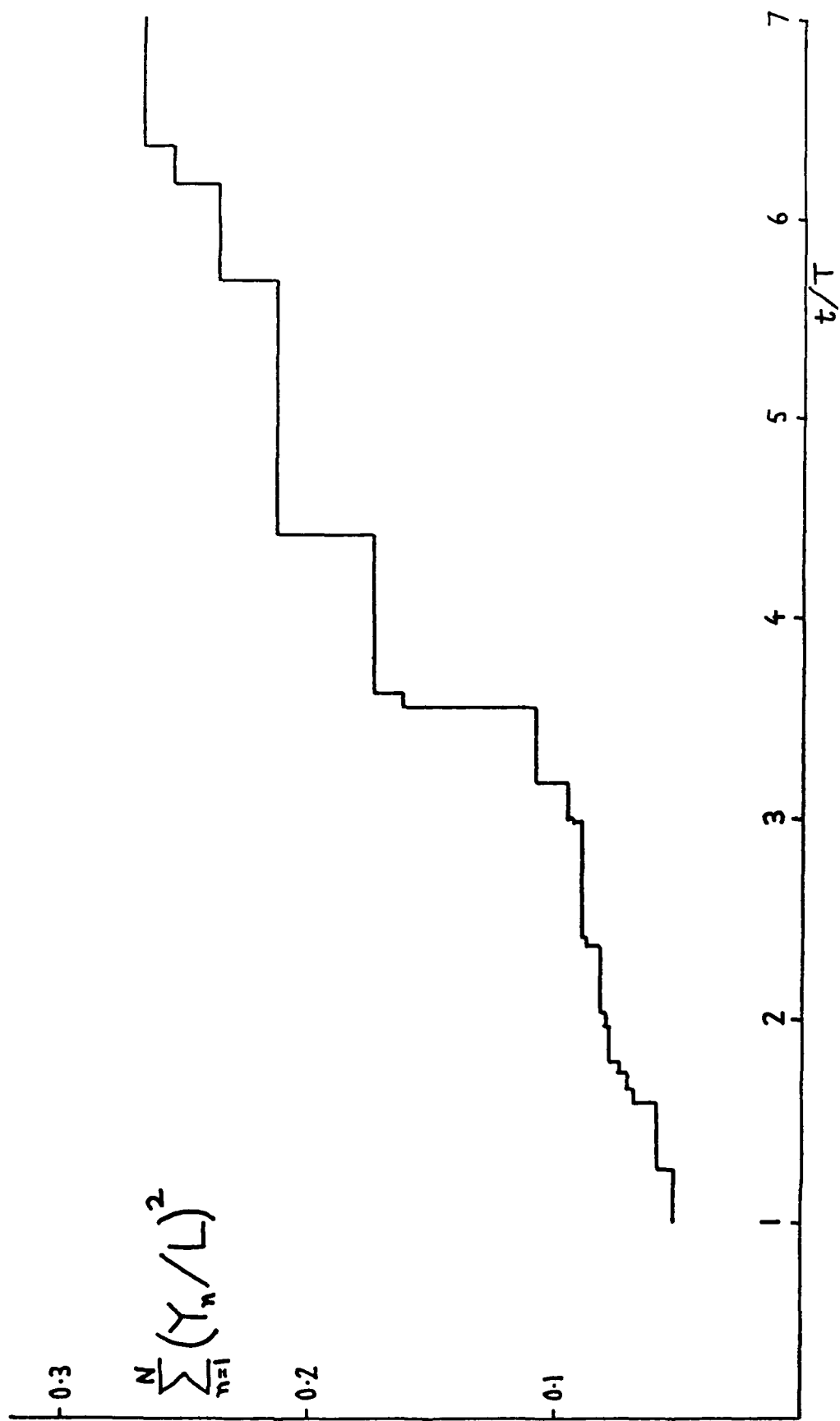


Figure 4.

REPORT DOCUMENTATION PAGE			Form Approved OMB No. 0704-0188	
<small>Public reporting burden for this collection of information is estimated to average 1 hour per response, including the time for reviewing instructions, searching existing data sources, gathering and maintaining the data needed, and completing and reviewing the collection of information. Send comments regarding this burden estimate or any other aspect of this collection of information, including suggestions for reducing this burden, to Washington Headquarters Services, Directorate for Information Operations and Reports, 1215 Jefferson Davis Highway, Suite 1204, Arlington, VA 22202-4302, and to the Office of Management and Budget, Paperwork Reduction Project (0704-0188), Washington, DC 20503.</small>				
1. AGENCY USE ONLY (Leave blank)		2. REPORT DATE May 1993		3. REPORT TYPE AND DATES COVERED Contractor Report
4. TITLE AND SUBTITLE SOME ASPECTS OF THE AEROACOUSTICS OF HIGH-SPEED JETS			5. FUNDING NUMBERS C NAS1-19480  WU 50-90-52-01	
6. AUTHOR(S)  James Lighthill				
7. PERFORMING ORGANIZATION NAME(S) AND ADDRESS(ES) Institute for Computer Applications in Science and Engineering Mail Stop 132C, NASA Langley Research Center Hampton, VA 23681-0001			8. PERFORMING ORGANIZATION REPORT NUMBER  ICASE Report No. 93-20	
9. SPONSORING/MONITORING AGENCY NAME(S) AND ADDRESS(ES) National Aeronautics and Space Administration Langley Research Center Hampton, VA 23681-0001			10. SPONSORING/MONITORING AGENCY REPORT NUMBER NASA CR-191458 ICASE Report No. 93-20	
11. SUPPLEMENTARY NOTES Langley Technical Monitor: Michael F. Card Final Report			Submitted to Theoretical and Computational Fluid Dynamics	
12a. DISTRIBUTION/AVAILABILITY STATEMENT  Unclassified - Unlimited Subject Category 34			12b. DISTRIBUTION CODE	
13. ABSTRACT (Maximum 200 words)  The Lecture begins by sketching some of the background to contemporary jet aeroacoustics. Then it reviews scaling laws for noise generation by low-Mach-number airflows and by turbulence convected at "not so low" Mach number. These laws take into account the influence of Doppler effects associated with the convection of aeroacoustic sources.  Next, a uniformly valid Doppler-effect approximation exhibits the transition, with increasing Mach number of convection, from compact-source radiation at low Mach numbers to a statistical assemblage of conical shock waves radiated by eddies convected at supersonic speed. In jets, for example, supersonic eddy convection is typically found for jet exit speeds exceeding twice the atmospheric speed of sound.  The Lecture continues by describing a new dynamical theory of the nonlinear propagation of such statistically random assemblages of conical shock waves. It is shown, both by a general theoretical analysis and by an illustrative computational study, how their propagation is dominated by a characteristic "bunching" process. That process - associated with a tendency for shock waves that have already formed unions with other shock waves to acquire an increased proneness to form further unions - acts so as to enhance the high-frequency part of the spectrum of noise emission from jets at these high exit speeds.				
14. SUBJECT TERMS jet acoustics, nonlinear propagation, conical shocks, numerical experiments			15. NUMBER OF PAGES 47	
			16. PRICE CODE A03	
17. SECURITY CLASSIFICATION OF REPORT Unclassified	18. SECURITY CLASSIFICATION OF THIS PAGE Unclassified	19. SECURITY CLASSIFICATION OF ABSTRACT	20. LIMITATION OF ABSTRACT	

NSN 7540-01-280-5500

Standard Form 298 (Rev 2-89)  
Prescribed by ANSI Std Z39-18  
298-102